scientific reports

Check for updates

OPEN

Transcriptome analysis of orbital tissue in thyroid eye disease uncovers key pathogenic mediators

Wumei Hua[1,2], Xiaolan Ji[1], Jingqiao Chen[1], Ziyuan Jiang[1], Honglin Chen[1], Yuhui Cui[3], Minyan Li[1,4], Xingyu Lu[5], Xuefeng Wang[1]✉ & Ji Zhang[1]✉

This study employed RNA sequencing and bioinformatics to identify differentially expressed genes (DEGs) and signaling pathways in thyroid eye disease (TED). Orbital adipose tissues from TED patients and normal controls were sequenced, followed by DEG screening. Primary cultured orbital fibroblasts were used to validate highly expressed DEGs via qRT-PCR. We observed significant upregulation of genes involved in adipogenesis (e.g., ACSL5), muscle fiber formation/contraction (e.g., TNNT1), and nerve injury (e.g., NEFM) in TED. qRT-PCR confirmed elevated expression of IL-6, COL1A1, PPARγ, NEFM, ACSL5, and TNNT1 in TED fibroblasts. Enrichment analysis revealed 20 significantly altered biological processes, including triglyceride biosynthesis and muscle filament sliding. Upregulated DEGs were primarily associated with the PPAR, AMPK, and adipocytokine signaling pathways. Our findings identify ACSL5, TNNT1, and NEFM as key mediators in TED pathogenesis, contributing to adipogenesis, muscle thickening, and nerve injury, respectively. The PPARγ-ACSL5 pathway is implicated in orbital adipogenesis, suggesting potential therapeutic targets for TED.

TED, also known as Graves' ophthalmopathy, is characterized by retrobulbar tissue inflammation, adipose hyperplasia, and fusiform hypertrophy of extraocular muscles, leading to orbital volume expansion and remodeling[1]. The pathogenesis of TED remains incompletely understood and involves mechanisms such as immune responses, apoptosis, and autophagy[2]. In TED's immune mechanism, interactions among fibroblasts, activated $CD4^+$ T cells, and cytokines may directly induce orbital inflammation, subsequently activating fibrosis and fat accumulation in the orbit, thereby contributing to TED development[3,4].

Transcriptome sequencing, as a representative high-throughput sequencing technology in recent years, enables the analysis of differential gene expression by comparing gene expression profiles from different tissues and conditions to identify genes that play a major role in phenotypes[5]. Studies have shown that analyzing differential gene expression in tumors is helpful in identifying potential cancer biomarkers[6–9]. Given the important role of transcriptome sequencing in various diseases, it is reasonable to believe that it can identify new molecular targets for TED and provide new insights for mechanistic research and potential treatment. Therefrom, a comprehensive analysis, combining transcriptome sequencing of TED patient orbital connective tissue with relevant Thyroid-Associated Ophthalmopathy datasets from the Gene Expression Omnibus (GEO), will be conducted to pinpoint potential novel differentially expressed genes and their underlying signaling pathways.

Materials and methods

Patients and samples

A total of 13 cases of orbital adipose connective tissue were obtained from patients with TED during orbital decompression surgery, and 12 cases of normal controls were obtained from the same tissue during oculoplastic surgery, matched for age and sex (Table 1). Transcriptome analysis was performed in three cases from the TED group and three cases from the control group. The study was conducted in accordance with the Declaration of

[1]Department of Ophthalmology, School of Basic Medical Sciences, The Second Affiliated Hospital of Soochow University, Suzhou Medical College of Soochow University, Suzhou 215004, People's Republic of China. [2]Department of Ophthalmology, Tongling People's Hospital, Tongling 244000, People's Republic of China. [3]Suzhou Xiangcheng People's Hospital, 215131 Suzhou, People's Republic of China. [4]Suzhou High School Affiliated to Xi'an Jiaotong University, Suzhou 215217, People's Republic of China. [5]School of Radiation Medicine and Protection, Suzhou Medical College of Soochow University, Suzhou 215123, People's Republic of China. ✉email: wangxuefeng@suda.edu.cn; jizhang@suda.edu.cn

	Patients with TED	Healthy subjects
Age(range)	55.15 ± 12.16	56.50 ± 19.23
Gender F/M	6/7	7/5
History of smoking	2/13	1/12
Clinical activity score		
< 3	5	-
≥ 3	8	-
Disease duration median(month)	6	-
Thyroid function		-
Hyperthyroid	6/13	0/12
Hypothyroid	0/13	0/12
Euthyroid	7/13	12/12

Table 1. Clinical profile of participants from TED patients and controls.

Helsinki and was approved by the Ethics Committee of the Second Affiliated Hospital of Soochow University, China.

Analysis of public TED gene expression data

We interrogated GEO database using the keyword "Thyroid associated Ophthalmopathy" and identified the dataset GSE58331 for analysis. This dataset, profiled on the Affymetrix Human Genome U133 Plus 2.0 Array (GPL570), included gene expression data from retrobulbar connective tissue and lacrimal glands across multiple cohorts. For our study, we selectively extracted data from retrobulbar connective tissues, excluding samples from lacrimal glands and orbits with nonspecific inflammation. The final curated dataset comprised 27 Thyroid-Associated Ophthalmopathy and 21 normal control samples.

RNA extraction and database construction

Total RNA was extracted using Trizol reagent according to the manufacturer's protocol. RNA purity and concentration were measured using a NanoDrop 2000 spectrophotometer (Thermo Scientific, USA), and RNA integrity was assessed with an Agilent 2100 Bioanalyzer (Agilent Technologies, Santa Clara, CA, USA). Libraries were constructed using the TruSeq Stranded mRNA LT Sample Prep Kit (Illumina, San Diego, CA, USA) according to the manufacturer's instructions. Transcriptome sequencing and analysis were performed by OE Biotech Co., Ltd. (Shanghai, China).

Cell culture

Orbital adipose connective tissue collected during surgery was placed in 100 mm Petri dishes containing DMEM supplemented with 20% FBS and 1% penicillin–streptomycin for primary fibroblast culture. Cells were continuously passaged, and those between the third and eighth passages were used for experiments.

qRT-PCR

Total RNA was extracted from cultured fibroblasts using a total RNA extraction kit and reverse transcribed into cDNA with a reverse transcription kit. qRT-PCR was performed using a PCR instrument. The primers used in this experiment are shown in Table 1, and GAPDH served as the internal reference.

Data analysis

Data were analyzed using the ΔΔCT method: ΔCT = CT value of target gene − CT value of internal reference gene; ΔΔCT = [ΔCT (experimental group)] − [ΔCT (mean value of control group)]; fold change = 2^(-ΔΔCT), representing the relative gene expression in the experimental group compared with the control group. Data were expressed as mean ± standard error, and independent-sample t-tests were performed for comparisons between groups. Statistical analysis and figure plotting were conducted using GraphPad Prism software. A P-value ≤ 0.05 was considered statistically significant.

Result

Identification and functional characterization of differentially expressed genes in TED

To identify genes differentially expressed in TED, we analyzed the "GSE58331" dataset from GEO. This analysis yielded 114 DEGs, of which 9 were upregulated and 105 were downregulated (Supplementary Fig. 1). Subsequently, functional enrichment analysis was conducted, which identified significant terms across biological processes, molecular functions and cellular components (Supplementary Fig. 2). Moreover, a protein-protein interaction network was constructed from the DEGs, pinpointing CD44, CD24, and SSR gene family members as potential key contributors to TED pathogenesis (Supplementary Fig. 3).

Identification of differentially expressed genes TED and normal control adipose tissues

To identify differentially expressed genes between TED and normal control adipose tissues from our obtained samples, we analyzed RNA-seq data with FPKM > 1 as the expression threshold. A Venn diagram showed 11,399 genes co-expressed in both groups, with 164 and 399 genes specific to the TED and control groups,

respectively (Fig. 1a). We then screened for statistically significant DEGs using DESeq2 with stringent criteria (|log2FC| ≥ 2 and FDR < 0.01), which identified 288 DEGs (198 upregulated, 90 downregulated). Notably, the most significantly upregulated genes (e.g., RPS4Y1, DDX3Y) and downregulated genes (e.g., FRZB, LGR5) are displayed in the heatmap and volcano plot (Fig. 1b and c).

Deciphering the transcriptional landscape underlying TED pathogenic mechanisms

TED pathogenesis involves activation of orbital inflammation, increased fat volume, and hypertrophy of extraocular muscles. Our data revealed significant differences in the expression of genes related to fat

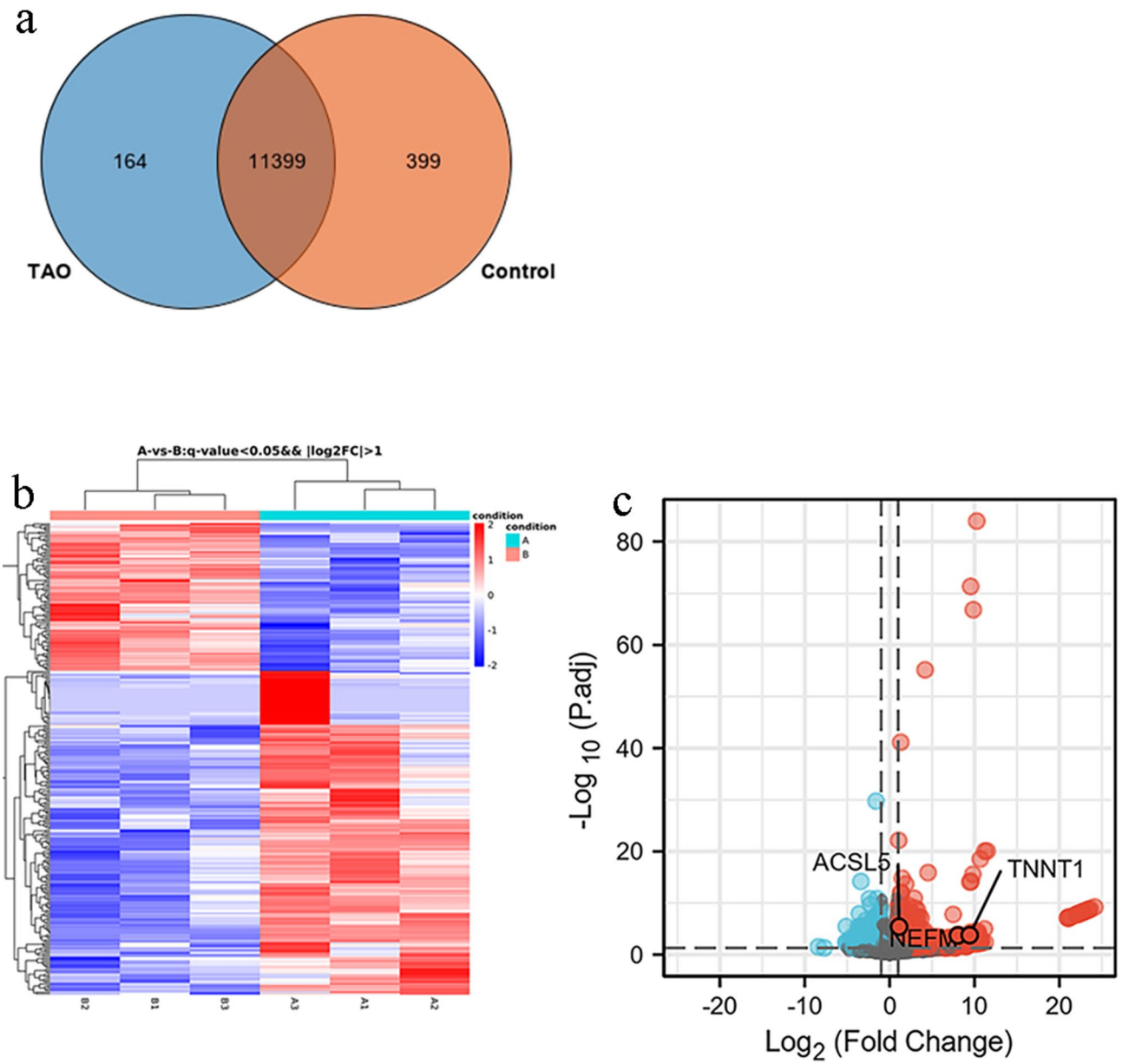

Fig. 1. Identification and functional characterization of differentially expressed genes in TED. **a** Wayne diagram shows the gene expression level of orbital connective tissue in TED and controls. The blue part indicates that there are 164 genes specifically expressed in TED, the orange part indicates that 399 genes are specifically expressed in controls, and the dark overlap indicates that there are 11,399 genes expressed between the two groups. **b** Heatmap from the hierarchical clustering analysis showed the differential expressed mRNAs between the two groups. The color scale on the top illustrates the relative expression level of mRNAs across all samples: red denotes mRNA expression greater than the average value, and blue denotes mRNA expression lesser than the average value. A: TED group, B:control group. **c** Volcano plots of all detected mRNAs in the TED and Control groups. The red dots represent significantly upregulated genes (log2 fold change > 1 and adjusted $P < 0.05$); the blue dots represent significantly downregulated genes (log2 fold change < − 1 and adjusted $P < 0.05$).

metabolism, including PCK2, ACSL5, GYS1, ACACA, FASN, ACADL, DGAT1, AQP7, and LPL, which were markedly expressed in TAO (Fig. 2a; Table 2). Muscle hypertrophy, as a contributing factor to proptosis in TED, can be detected based on orbital Computed Tomography (CT). Consistent with this, genes related to muscle fiber formation and contraction such as TNNT1, MYL1, MYH2, and ACTC1, were highly expressed in TED, with some not expressed at all in controls (Fig. 2b; Table 3). These highly specific genes may play a decisive role in fusiform hypertrophy of orbital muscles. Additionally, genes related to nerve growth and function showed decreased expression in TED compared with controls (Fig. 2c; Table 4). Specifically, NELL2, GFRA2, NTNG1, and PPFIA2, which are genes involved in neuronal growth, differentiation, and axon development, were downregulated, whereas NEFM, a biomarker of neuronal injury, was highly expressed in TED. These findings may provide a new direction for studying neurological impairment in TED.

Functional and pathway enrichment analysis of TED transcriptome

To delineate the functional landscape of TED, we performed Gene Ontology (GO) enrichment analysis. The results showed that highly expressed genes in TED were mainly involved in triglyceride biosynthetic process, muscle filament sliding, retinol metabolic process, diacylglycerol biosynthetic process, and fatty acid biosynthetic process. These genes were predominantly located in the myosin complex, myosin filament, lipid droplets, myofibril, sarcomere, extracellular exosome, extracellular space, and specific granule lumen, indicating that TED pathophysiology is largely associated with fat accumulation and muscle hypertrophy (Fig. 3a). In contrast, downregulated genes were mainly associated with collagen fibril organization, extracellular matrix organization, leukocyte migration, thyroid hormone generation, cell adhesion, and response to cAMP (Fig. 3b).

In parallel, Kyto Encyclopedia of Genes and Genomes (KEGG) pathway analysis showed that upregulated genes were mainly enriched in the PPAR signaling pathway, AMPK signaling pathway, and adipocytokine signaling pathway (Fig. 4a). Downregulated genes were mainly enriched in cell adhesion molecules, ECM–receptor interaction, PI3K-AKT signaling pathway, neuroactive ligand–receptor interaction, and cAMP signaling pathway (Fig. 4b).

These findings collectively underscore the involvement of specific metabolic and structural pathways in TED pathogenesis.

TED fibroblasts exhibit overexpression of key pathogenic factors

To validate our transcriptomic findings at the functional level, we quantified the expression of pivotal mediators in primary orbital fibroblasts. qRT-PCR demonstrated that TED fibroblasts significantly overexpressed the pro-inflammatory factor IL-6, the profibrotic gene COL1A1, and the lipogenic transcription factor PPARγ relative to normal fibroblasts (Fig. 5a).

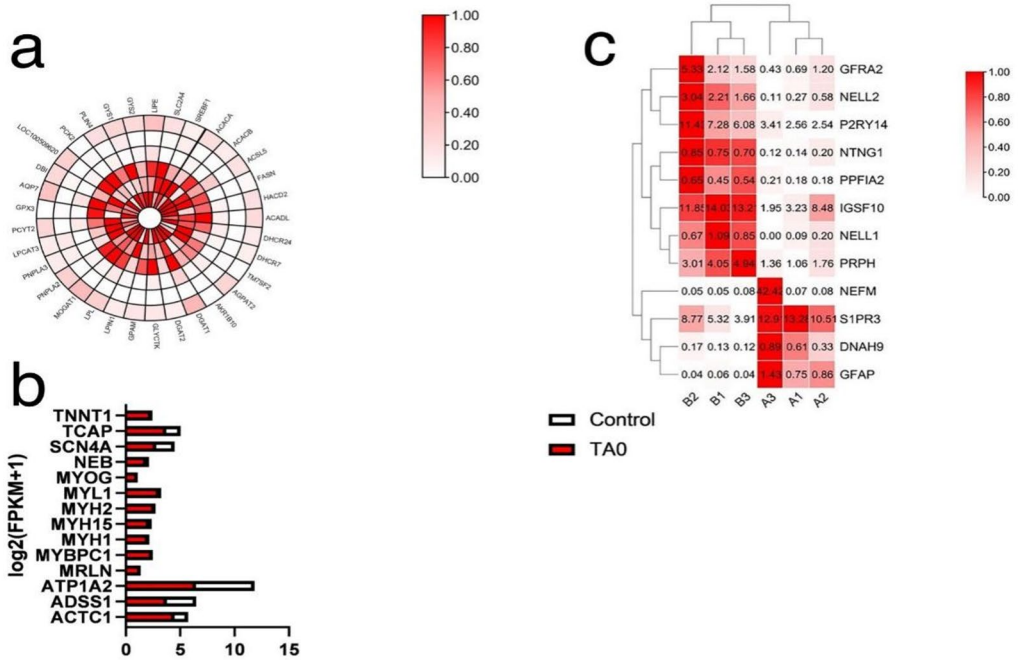

Fig. 2. Identification of differentially expressed genes TED and normal control adipose tissues. **a** Genes related to adipogenesis. The color shades represent the level of gene expression, and the inner circle to outer circle are A1, A2, A3, B1, B2 and B3 in total 6 groups of specimens. **b** Genes related to muscle fibers. Red represents TED group and white represents control group. **c** Genes related to nerve growth and function. The darker the red, the more significant the difference. A1-A3 represent the TED group and B1-B3 represent normal controls.

gene_id	Location	log2FoldChange	*p*-value	q-value
ACACA	chr17:17q12	1.323781593	4.46E-05	3.75E-03
ACACB	chr12:12q24.11	1.260489566	2.77E-04	1.52E-02
ACSL5	chr10:10q25.2	1.110111431	3.93E-06	5.00E-04
FASN	chr17:17q25.3	4.175522541	6.50E-56	2.61E-52
HACD2	chr3:3q21.1	1.197355056	1.72E-04	1.10E-02
ACADL	chr2: 2q34	1.373325138	4.95E-11	3.18E-08
DHCR24	chr1:1p32.3	1.464135551	1.57E-15	1.93E-12
TM7SF2	chr11: 11q13.1	1.146520283	7.51E-09	2.36E-06
AGPAT2	chr9:9q34.3	1.135557902	4.26E-05	3.65E-03
AKR1B10	chr7:7q33	4.072252121	1.97E-05	1.97E-03
DGAT2	chr11:11q13.5	2.271904886	3.94E-07	7.44E-05
GLYCTK	chr3:3p21.2	1.885885052	6.52E-07	1.14E-04
GPAM	chr10:10q25.2	1.72075088	2.10E-07	4.38E-05
LPIN1	chr2:2p25.1	1.047993899	1.59E-03	4.98E-02
LPL	chr8:8p21.3	1.446382931	1.60E-06	2.25E-04
MOGAT1	chr2:2q36.1	1.665991128	7.05E-04	2.93E-02
PNPLA2	chr11:11p15.5	1.382585181	5.37E-07	9.57E-05
PNPLA3	chr22:22q13.31	2.399586737	9.26E-05	6.63E-03
LPCAT3	chr12:12p13.31	1.32782571	9.31E-07	1.45E-04
PCYT2	chr17: 17q25.3	1.252008911	1.13E-06	1.70E-04
GPX3	chr5:5q33.1	2.416516231	9.99E-07	1.54E-04
AQP7	chr9:9p13.3	1.245194186	2.78E-05	2.61E-03
DBI	chr2:2q14.2	1.176075314	7.36E-07	1.25E-04
LOC100509620	chr2:2q11.1	1.871628975	1.95E-04	1.20E-02
PCK2	chr14:14q11.2-q12	1.06447549	7.64E-04	3.07E-02
PLIN4	chr19:19p13.3	1.113032723	1.52E-03	4.84E-02
GYS1	chr19:19q13.33	1.073895224	6.17E-04	2.65E-02
GYS2	chr12:12p12.1	2.144001154	2.18E-04	1.30E-02
LIPE	chr19:19q13.2	1.043989096	1.95E-04	1.20E-02
SLC2A4	chr17:17p13.1	2.149041209	2.82E-10	1.51E-07
SREBF1	chr17:17p11.2	1.892446614	2.24E-14	2.11E-11

Table 2. Summary of fat-related genes.

gene-ID	Location	log2FoldChange	*p*-value	q-value
ACTC1	chr15:15q14	8.057867	1.07E-04	7.49E-03
ADSS1	chr14:14q32.33	1.413728	1.84E-04	1.16E-02
ATP1A2	chr1:1q23.2	1.139146	5.16E-04	2.37E-02
MRLN	chr10:10q21.2	22.14722	1.45E-08	4.23E-06
MYBPC1	chr12:12q23.2	10.54961	2.56E-04	1.44E-02
MYH1	chr17:17p13.1	8.44066	2.59E-04	1.45E-02
MYH15	chr3:3q13.13	7.124153	4.65E-04	2.21E-02
MYH2	chr17:17p13.1	11.17272	1.04E-05	1.15E-03
MYL1	chr2:2q34	10.38719	3.39E-05	3.07E-03
MYOG	chr1:1q32.1	21.13791	6.34E-08	1.47E-05
NEB	chr2:2q23.3	6.561484	1.21E-03	4.13E-02
SCN4A	chr17:17q23.3	1.629126	3.59E-0	1.83E-02
TCA	chr17:17q12	6.809576	6.49E-04	2.77E-02
TNNT1	chr19:19q13.42	9.430121	1.70E-04	1.10E-02

Table 3. Summary of genes related to muscle fiber.

gene-ID	Location	log2FoldChange	*p*-value	q-value
DNAH9	Chr17: 17p12	2.229453	1.30E-06	1.92E-04
GFAP	Chr17: 17q21.31	4.525004	1.31E-16	1.91E-13
GFRA2	Chr8: 8p21.3	−1.90736	6.49E-04	2.77E-02
IGSF10	Chr3: 3q25.1	−1.46734	1.05E-03	3.86E-02
NEFM	Chr8: 8p21.2	8.041277	1.95E-04	1.20E-02
NELL1	Chr11.:11p15.1	−3.1313	1.48E-04	9.84E-03
NELL2	Chr12: 12q12	−2.80615	2.53E-07	5.13E-05
NTNG1	Chr1: 1p13.3	−2.26179	2.14E-10	1.22E-07
P2RY14	Chr3: 3q25.1	−1.45981	4.77E-06	5.72E-04
PPFIA2	Chr12: 12q21.31	−1.43342	4.32E-05	3.66E-03
PRPH	Chr12: 12q13.12	−1.44887	1.46E-05	1.52E-03
S1PR3	Chr9: 9q22.1	1.113176	7.18E-04	2.96E-02

Table 4. Summary of differential genes related to nerve damage.

Validation of key differentially expressed genes in orbital fibroblasts

Based on our transcriptomic profiling, we selected three candidate genes including NEFM (neuronal injury), ACSL5 (lipogenesis) and TNNT1 (muscle contraction) from the 288 identified DEGs for further validation. qRT-PCR analysis in primary cultured orbital fibroblasts confirmed significantly elevated expression of all three genes in the TED group compared to normal controls ($p < 0.05$), which was consistent with the transcriptome sequencing data (Fig. 5b).

Discussion

The rising standard of living and increased focus on personal health have contributed to earlier diagnosis of TED, which predominantly affects women aged 30–50 years, with an overall prevalence of 0.5%[10]. Understanding its pathogenesis and identifying molecular targets remain central to ophthalmology research. Current investigations focus on TSHR and IGF-1R as key molecular targets. While TSHR is central to hyperthyroidism, its role in TED remains controversial due to its low expression in orbital tissues compared to thyroid epithelial cells[11,12]. IGF-1R has attracted attention with the approval of teprotumumab for active TED[13,14]. However, the mechanisms underlying refractory fat accumulation and muscle thickening in TED, particularly in the absence of marked inflammation, remain poorly understood.

Advances in high-throughput sequencing and multi-omics approaches have enabled comprehensive biomarker discovery across diseases, including cancer and autoimmune disorders[15–17]. For instance, Zhang et al. synthesized multi-omics advances in TED, highlighting biomarker potential across genomic, transcriptomic, proteomic, metabolomic and microbiomic domains[17]. Marinò et al. identified epigenetic mechanisms as pivotal in driving differential gene expression in TED[18]. Proteomic studies have further nominated upregulated proteins involved in inflammation and tissue remodeling as biomarkers of disease severity[19], while single-cell sequencing has delineated the local cellular landscape, informing therapeutic strategies[20].

In this study, transcriptomic analysis of orbital adipose tissue from TED patients and normal controls identified 288 differentially expressed genes (198 upregulated, 90 downregulated), largely involved in fat metabolism. These findings align with the metabolic profiling by Huang et al.[21], who reported alterations in cholesterol metabolism, adipocyte lipolysis and insulin resistance. Reduced Thy1 expression in TED fibroblasts suggests a shift toward adipogenic differentiation, as Thy-1$^+$ fibroblasts preferentially differentiate into adipose fibroblasts[2,22,23], potentially driving orbital fat accumulation.

Orbital fibroblasts (OFs) serve as central mediators in TED, driving progression through multiple mechanisms. They are activated by cytokines from infiltrating inflammatory cells, triggering phenotypically distinct populations[3,24,25]. Single-cell transcriptomic profiling of TED orbital tissue has further defined a specific PDGFRα + DPP4 + fibroblast subpopulation. This subset demonstrates both progenitor-like attributes and a marked propensity for fibrosis, thereby establishing its pivotal role in driving the fibrotic remodeling of the orbit[26]. In this study, primary OFs from orbital adipose tissue exhibited elevated expression of IL-6, COL1A1, and PPARγ, consistent with earlier findings. Burnstine et al.[27] confirmed high IL-6 mRNA in OFs, and recent evidence shows that TED-related proteins further enhance IL-6 expression. PPARs, nuclear hormone receptors with three subtypes (PPARα, PPARγ, and PPARβ/δ), regulate energy metabolism[28]. PPARγ is essential for adipose tissue development and adipogenic differentiation of fibroblasts and stem cells[29,30]. Its immunomodulatory role is well established. For example, Kumar et al.[31] correlated PPARγ levels in TED tissue with adipogenesis and TSHR expression. Consistent with this, single-cell RNA sequencing (sc-RNA seq) by Kim et al.[32] revealed an expanded adipogenic fibroblast fraction in TED orbits, aligning with our PPARγ upregulation. PPARα has also been implicated in inflammation by modulating CXCL8 and CXCL10 secretion in OFs and preadipocytes[28,33]. We further observed high COL1A1 expression, supporting its role in orbital fibrosis. Together, these results collectively establish OFs as key drivers of inflammation, fibrosis, and adipogenesis in TED via dysregulation of IL-6, PPARγ and COL1A1.

We selected three representative genes, NEFM, ACSL5, and TNNT1, which were from our transcriptomic data, and confirmed their elevated expression in TED orbital fibroblasts, supporting the reliability of our

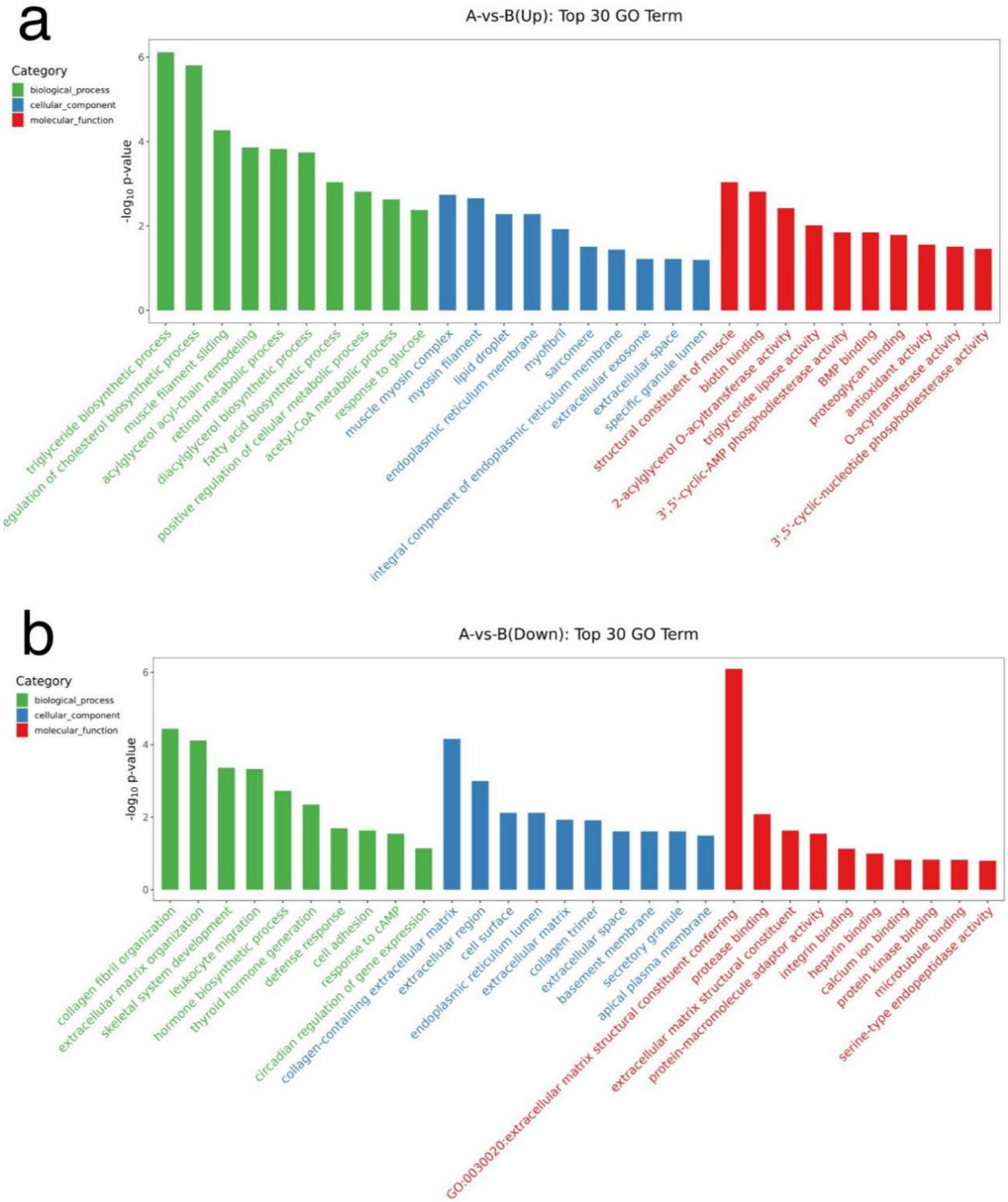

Fig. 3. Gene ontology enrichment analysis. Upregulated **(a)** and downregulated **(b)** genes. The highly expressed genes in TED group are mainly involved in the triglyceride biosynthetic process, while the low expressed genes are mainly involved in the collagen fibril organization. A: TED group, B: control group.

sequencing results. ACSL5, a member of the acyl-CoA synthetase family, mediates de novo lipogenesis, fatty acid degradation, and membrane remodeling[34]. Substrate specificity among acyl-CoA synthetases, which include ACSL1, ACSL3, ACSL4, ACSL5 and ACSL6[35], depends on fatty acid carbon chain length (C12–C20). Although ACSL5 has been implicated in tumor progression, serving as a favorable prognostic marker in pancreatic cancer[36] yet exerting oncogenic effects in gastric cancer[37], its role in TED remains unstudied. Notably, ACSL5 is a transcriptional target of SREBP1-c[38], PPARα[39] and PPARγ[40]. Given the significant enrichment of PPAR signaling in TED and the co-upregulation of both PPARγ and ACSL5 in fibroblasts, we propose that the PPARγ/ACSL5 axis may contribute to orbital adipogenesis in TED.

We observed significant upregulation of genes involved in muscle fiber formation and contraction including MYL1, MYH1, MYH2, MYH15, NEB, TCAP, and TNNT1, consistent with previous reports[41]. It has been proposed that myogenesis may be associated with the increased muscle volume in the early stage of the disease and its correlation with the severity of TED[42].GO analysis further confirmed significant enrichment of muscle

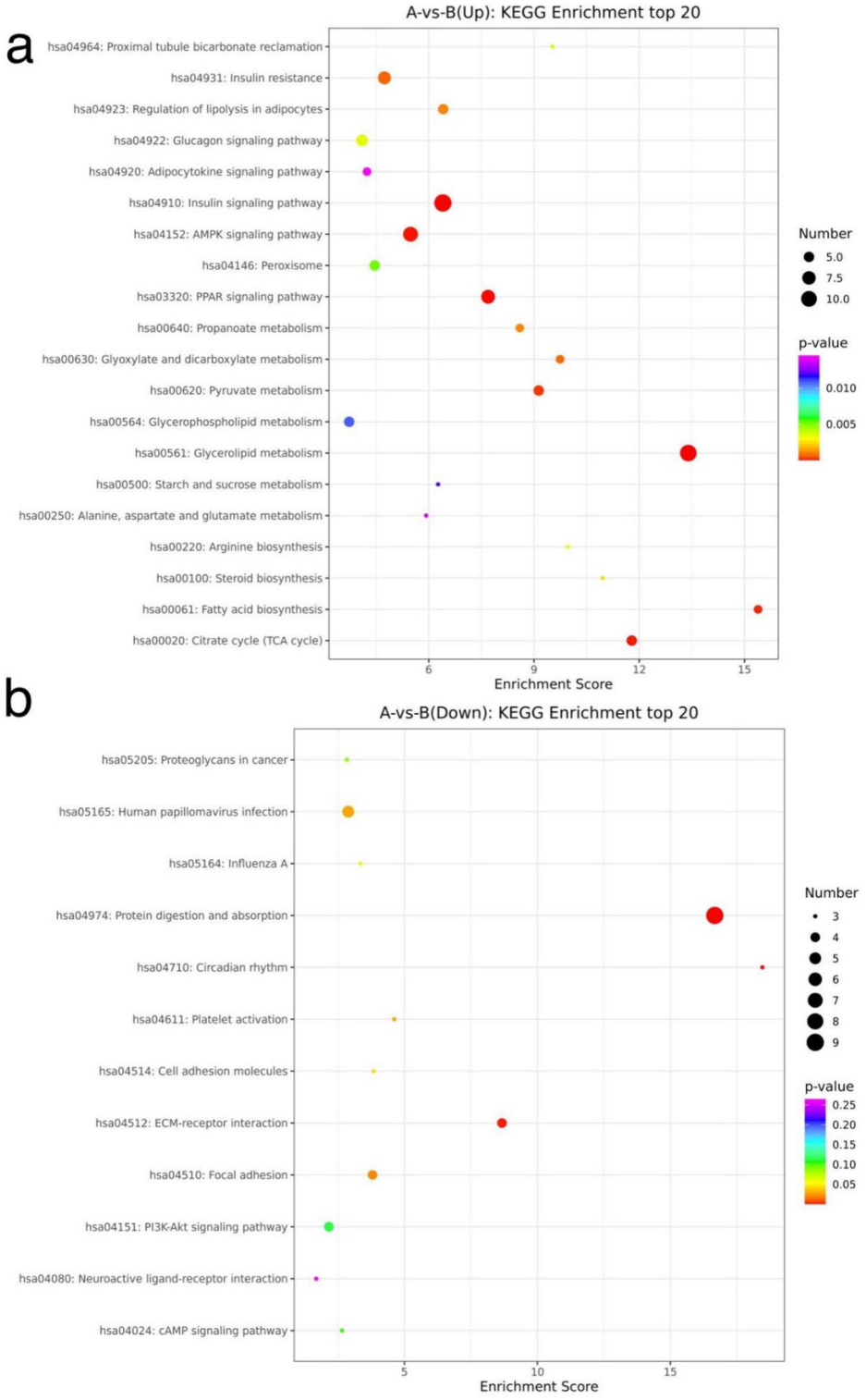

Fig. 4. KEGG analysis of the biological pathways. Upregulated **(a)** and downregulated **(b)** genes. The color scale on the top right shows the relative expression level of the genes and the size of the open circle on the lower right represents the number of genes.

structure organization and muscle filament sliding in TED. Myosin heavy chain isoforms, which regulate muscle fiber contractility, are predominantly composed of MYH1, MYH2, and MYH13 in healthy extraocular muscles[43]. In addition to MYH1 and MYH2, our study identified MYL1 involvement in myosin assembly. We also detected elevated expression of ATP1A2 and SCN4A, implicated in neuromuscular action potential, along with TNNT1, which regulates muscle contraction. These findings collectively suggest that dysregulated expression of TNNT1,

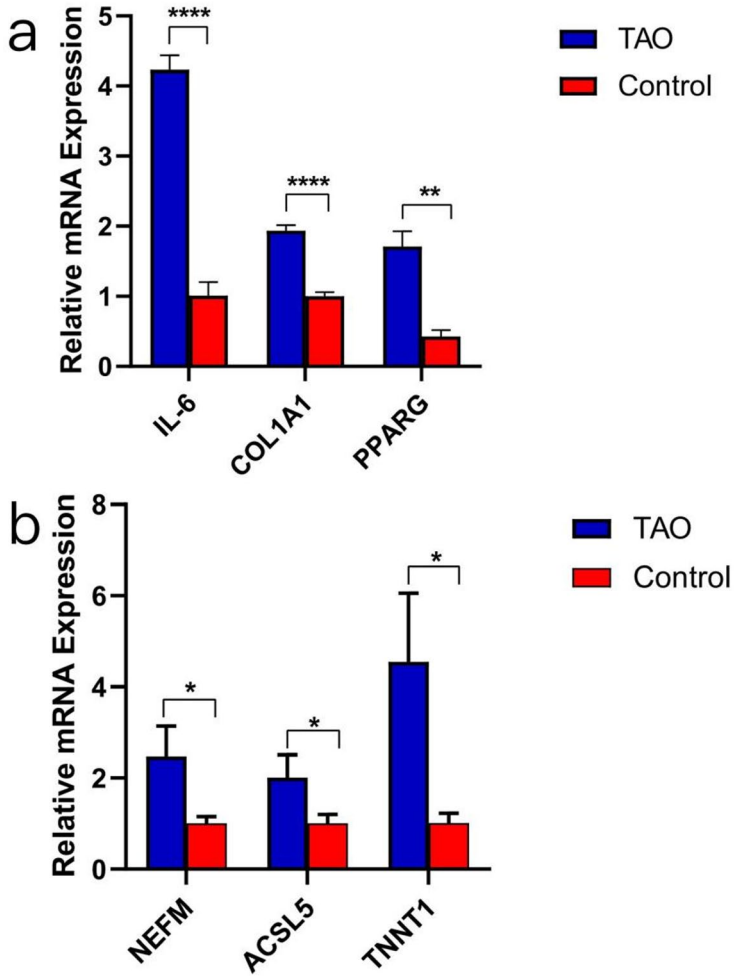

Fig. 5. Validation of key differentially expressed genes in orbital fibroblasts **a** The cultured primary fibroblasts were detected by qRT-PCR. The orbital fibroblasts in TED group expressed high levels of IL-6 pro-inflammatory factor, COL1A1 fibrosis factor and PPAR-γ lipid-promoting factor. **b** Three genes with large differences and high expression abundance in the sequencing results were selected for verification. NEFM, ACSL5 and TNNT1 were highly expressed in TED orbital fibroblasts, and the p value was <0.05. The difference was statistically significant. Blue is TED group, red is control group. Data are presented as mean ± SD ($n=13$ per TED and 12 per control). $^{*}P<0.05$, $^{**}P<0.01$ and $^{****}P<0.0001$.

MYH1, MYH2, MYL1, SCN4A, and ATP1A2 may alter contractile properties of extraocular muscles in TED. Subsequent validation experiments confirmed elevated TNNT1 expression in TED orbital fibroblasts.

Transcriptomic analysis revealed a distinct neural expression profile in TED orbits. Genes involved in nerve development were downregulated, while those associated with nerve injury were elevated. Specifically, NELL2 and GFRA2 (neuronal growth/differentiation) and NTNG1 and PPFIA2 (axonal development) showed reduced expression, whereas NEFM, a recognized biomarker of neuronal injury, was markedly upregulated in TED fibroblasts. As neurodevelopmental injury pathways have not been previously reported in TED, these findings suggest that orbital nerve impairment may precede mechanical compression from increased orbital volume. These genes may thus offer new insights into TED pathogenesis.

We also noted significant downregulation of extracellular matrix (ECM)-related genes, which contrasts with the elevated expression of fibrotic proteins commonly reported in TED. This observation aligns with previous transcriptomic studies describing impaired ECM organization and cell adhesion in TED. For example, Wu et al.[44] reported that downregulated mRNAs in TED were predominantly linked to cell adhesion, collagen catabolism, and ECM organization.

Functional enrichment analyses provided further insights into TED pathogenesis. GO and KEGG results collectively identified adipogenesis, muscle fiber formation, nerve injury, and extracellular matrix reorganization as core pathological processes in TED. Specifically, GO analysis revealed significant enrichment of lipid metabolic processes including triglyceride, cholesterol, diglyceride and fatty acid biosynthesis, alongside retinol metabolism and BMP binding, findings consistent with previous transcriptomic studies[44–46]. KEGG pathway analysis demonstrated enrichment in PPAR, AMPK, insulin, and adipocytokine signaling pathways, all implicated in adipogenic regulation. To address limitations from the small sequencing cohort, we supplemented

our analysis with a public TED microarray dataset from GEO. This external validation identified 9 upregulated and 105 downregulated genes, with enrichment in biological processes including retinal homeostasis, neutrophil degranulation, and ECM organization. Integration of this independent dataset thus reinforced and extended our primary findings, providing a more comprehensive view of TED pathology.

In summary, our findings implicate ACSL5, TNNT1, and NEFM as key mediators of adipogenesis, extraocular muscle thickening, and neuropathic injury in TED. The elevated expression of these genes in TED orbital fibroblasts underscores their pathogenic significance. Specifically, the PPARγ–ACSL5 signaling axis emerges as a potential driver of orbital adipogenesis. Future studies should prioritize experimental validation of this pathway, with the broader goal of advancing mechanism-based therapies for TED.

Data availability

The data has been submitted to GEO with the accession number GSE308553.

Received: 22 September 2025; Accepted: 26 November 2025
Published online: 08 December 2025

References

1. Taylor, P. N. et al. New insights into the pathogenesis and nonsurgical management of graves orbitopathy. *Nat. Rev. Endocrinol.* **16** (2), 104–116 (2020).
2. Chiu, H. I., Wu, S. B. & Tsai, C. C. The role of fibrogenesis and extracellular matrix proteins in the pathogenesis of graves' ophthalmopathy. *Int. J. Mol. Sci.* **25** (6), 3288 (2024).
3. Buonfiglio, F., Ponto, K. A., Pfeiffer, N., Kahaly, G. J. & Gericke, A. Redox mechanisms in autoimmune thyroid eye disease. *Autoimmun. Rev.* **23** (5), 103534 (2024).
4. Khong, J. J., McNab, A. A., Ebeling, P. R., Craig, J. E. & Selva, D. Pathogenesis of thyroid eye disease: review and update on molecular mechanisms. *Br. J. Ophthalmol.* **100** (1), 142–150 (2016).
5. Finotello, F. & Di Camillo, B. Measuring differential gene expression with RNA-seq: challenges and strategies for data analysis. *Brief. Funct. Genomics*. **14** (2), 130–142 (2015).
6. Govindarajan, M., Wohlmuth, C., Waas, M., Bernardini, M. Q. & Kislinger, T. High-throughput approaches for precision medicine in high-grade serous ovarian cancer. *J. Hematol. Oncol.* **13** (1), 134 (2020).
7. Togni, M. et al. Identification of the NUP98-PHF23 fusion gene in pediatric cytogenetically normal acute myeloid leukemia by whole-transcriptome sequencing. *J. Hematol. Oncol.* **8**, 69 (2015).
8. Xu, H., Wang, C., Song, H., Xu, Y. & Ji, G. RNA-Seq profiling of circular RNAs in human colorectal cancer liver metastasis and the potential biomarkers. *Mol. Cancer*. **18** (1), 8 (2019).
9. Ye, H. et al. CD4 T-cell transcriptome analysis reveals aberrant regulation of STAT3 and Wnt signaling pathways in rheumatoid arthritis: evidence from a case-control study. *Arthritis Res. Ther.* **17** (1), 76 (2015).
10. Taylor, P. N. et al. Global epidemiology of hyperthyroidism and hypothyroidism. *Nat. Rev. Endocrinol.* **14** (5), 301–316 (2018).
11. Feliciello, A. et al. Expression of thyrotropin-receptor mRNA in healthy and graves' disease retro-orbital tissue. *Lancet* **342** (8867), 337–338 (1993).
12. Agretti, P. et al. Real-time PCR provides evidence for Thyrotropin receptor mRNA expression in orbital as well as in extraorbital tissues. *Eur. J. Endocrinol.* **147** (6), 733–739 (2002).
13. Douglas, R. S. et al. Teprotumumab for the treatment of active thyroid eye disease. *N Engl. J. Med.* **382** (4), 341–352 (2020).
14. Slentz, D. H., Nelson, C. C. & Smith, T. J. Teprotumumab: a novel therapeutic monoclonal antibody for thyroid-associated ophthalmopathy. *Expert Opin. Investig. Drugs*. **29** (7), 645–649 (2020).
15. Akhoundova, D. & Rubin, M. A. Clinical application of advanced multi-omics tumor profiling:shaping precision oncology of the future. *Cancer Cell.* **40** (9), 920–938 (2022).
16. Zhang, Y. & Lee, T. Y. Revealing the immune heterogeneity between systemic lupus erythematosus and rheumatoid arthritis based on Multi-Omics data analysis. *Int. J. Mol. Sci.* **23** (9), 5166 (2022).
17. Zhang, H. et al. Multi-OmicsApproaches to discover biomarkers of thyroid eye disease: A systematic review. *Int. J. Biol. Sci.* **20** (15), 6038–6055 (2024).
18. Marinò, M. et al. Role of genetics and epigenetics in graves' orbitopathy. *Eur. Thyroid J.* **13** (6), e240179 (2024).
19. Hai, Y. et al. High-Throughput Proteomics and Immunohistochemistry of Orbital Connective Tissue in Graves' Orbitopathy. *J. Clin. Endocrinol. Metab.* **21**, dgaf299 (2025 May).
20. Li, Z. et al. Single-cell RNA sequencing depicts the local cell landscape in thyroid-associated ophthalmopathy. *Cell. Rep. Med.* **3** (8), 100699 (2022).
21. Huang, J. et al. Integrative metabolic analysis of orbital adipose/connective tissue in patients with thyroid-associated ophthalmopathy. *Front. Endocrinol. (Lausanne)*. **13**, 1001349 (2022).
22. Koumas, L., Smith, T. J., Feldon, S., Blumberg, N. & Phipps, R. P. Thy-1 expression in human fibroblast subsets defines myofibroblastic or lipofibroblastic phenotypes. *Am. J. Pathol.* **163** (4), 1291–1300 (2003).
23. Smith, T. J. & Janssen, J. A. M. J. L. Insulin-like growth Factor-I receptor and Thyroid-Associated ophthalmopathy. *Endocr. Rev.* **40** (1), 236–267 (2019).
24. Smith, T. J. Unique properties of orbital connective tissue underlie its involvement in graves' disease. *Minerva Endocrinol.* **28** (3), 213–222 (2003).
25. Bahn, R. S. Graves' ophthalmopathy. *N Engl. J. Med.* **362** (8), 726–738 (2010).
26. Cheng, L. et al. PDGFRα + DPP4 + Fibroblasts-Macrophage crosstalk induces orbital fibrosis in Treatment-Resistant thyroid eye disease via the GAS6-AXL pathway. *Adv. Sci. (Weinh)*. **29**, e11404 (2025 Sep).
27. Burnstine, M. A., Elner, S. G., Strieter, R. M., Kunkel, S. L. & Elner, V. M. Orbital fibroblast interleukin-6 gene expression and Immunomodulation. *Ophthalmic Plast. Reconstr. Surg.* **15** (5), 306–311 (1999).
28. Christofides, A., Konstantinidou, E., Jani, C. & Boussiotis, V. A. The role of peroxisome proliferator-activated receptors (PPAR) in immune responses. *Metabolism* **114**, 154338 (2021).
29. Rosen, E. D. et al. PPAR gamma is required for the differentiation of adipose tissue in vivo and in vitro. *Mol. Cell.* **4** (4), 611–617 (1999).
30. Tontonoz, P., Hu, E. & Spiegelman, B. M. Stimulation of adipogenesis in fibroblasts by PPAR gamma 2, a lipid-activated transcription factor. *Cell* **79** (7), 1147–1156 (1994).
31. Kumar, S., Coenen, M. J., Scherer, P. E. & Bahn, R. S. Evidence for enhanced adipogenesis in the orbits of patients with graves' ophthalmopathy. *J. Clin. Endocrinol. Metab.* **89** (2), 930–935 (2004).
32. Kim, D. W. et al. Transcriptomic profiling of thyroid eye disease orbital fat demonstrates differences in adipogenicity and IGF-1R pathway. *JCI Insight*. **9** (24), e182352 (2024).

33. Ferrari, S. M. et al. Differential modulation of CXCL8 versus CXCL10, by cytokines, PPAR-gamma, or PPAR-alpha agonists, in primary cells from graves' disease and ophthalmopathy. *Autoimmun. Rev.* **18** (7), 673–678 (2019).
34. Meller, N., Morgan, M. E., Wong, W. P., Altemus, J. B. & Sehayek, E. Targeting of Acyl-CoA synthetase 5 decreases jejunal fatty acid activation with no effect on dietary long-chain fatty acid absorption. *Lipids Health Dis.* **12**, 88 (2013).
35. Klaus, C., Jeon, M. K., Kaemmerer, E. & Gassler, N. Intestinal acyl-CoA synthetase 5: activation of long chain fatty acids and behind. *World J. Gastroenterol.* **19** (42), 7369–7373 (2013).
36. Ma, W. et al. LOX and ACSL5 as potential relapse markers for pancreatic cancer patients. *Cancer Biol. Ther.* **20** (6), 787–798 (2019).
37. Quan, J., Bode, A. M. & Luo, X. ACSL family: the regulatory mechanisms and therapeutic implications in cancer. *Eur. J. Pharmacol.* **909**, 174397 (2021).
38. Kolehmainen, K. Kätilö ammatinharjoittajana [Kätilö ammatinharjoittajana [the profession of midwifery]. Katilolehti. ;97(2):3. Finnish, Swedish. (1992).
39. Boyd, J. E. & James, K. Human monoclonal antibodies: their potential, problems, and prospects. *Adv. Biotechnol. Processes*. **11**, 1–43 (1989).
40. Adamo, K. B. et al. Peroxisome proliferator-activated receptor gamma 2 and acyl-CoA synthetase 5 polymorphisms influence diet response. *Obes. (Silver Spring)*. **15** (5), 1068–1075 (2007).
41. Wu, L. et al. Integrative transcriptomics and proteomic analysis of extraocular muscles from patients with thyroid-associated ophthalmopathy. *Exp. Eye Res.* **193**, 107962 (2020).
42. Potgieser, P. W., Wiersinga, W. M., Regensburg, N. I. & Mourits, M. P. Some studies on the natural history of graves' orbitopathy: increase in orbital fat is a rather late phenomenon. *Eur. J. Endocrinol.* **173** (2), 149–153 (2015).
43. Kjellgren, D., Thornell, L. E., Andersen, J. & Pedrosa-Domellöf, F. Myosin heavy chain isoforms in human extraocular muscles. *Invest. Ophthalmol. Vis. Sci.* **44** (4), 1419–1425 (2003).
44. Wu, L. et al. Differential expression and alternative splicing of transcripts in orbital adipose/connective tissue of thyroid-associated ophthalmopathy. *Exp. Biol. Med. (Maywood)*. **246** (18), 1990–2006 (2021).
45. Chiquet, M., Birk, D. E., Bönnemann, C. G., Koch, M. & Collagen, X. I. I. Protecting bone and muscle integrity by organizing collagen fibrils. *Int. J. Biochem. Cell. Biol.* **53**, 51–54 (2014).
46. Kim, D. W. et al. Transcriptomic profiling of control and Thyroid-Associated orbitopathy (TAO) orbital fat and TAO orbital fibroblasts undergoing adipogenesis. *Invest. Ophthalmol. Vis. Sci.* **62** (9), 24 (2021).

Author contributions

Wumei Hua conceptualized and designed the study, collected and analyzed the data, drafted and wrote the initial manuscript, and critically reviewed and revised the manuscript. Xiaolan Ji and Jingqiao Chen critically reviewed the manuscript. Ziyuan Jiang, Honglin Chen, Minyan Li and Xingyu Lu conceptualized and designed the study, collected the data. Yuhui Cui collected and registered a subset of the specimens.Ji Zhang and Xuefeng Wang conceptualized and designed the study, collected and analyzed the data, drafted the initial manuscript, and critically reviewed and revised the manuscript. All authors approved the final manuscript as submitted and agreed to be accountable for all aspects of the work.

Funding

This work was funded by Jiangsu Provincial Natural Science Foundation Project (BK20231201), a project funded by the Priority Academic Program Development of Jiangsu Higher Education Institutions, the Project of State Key Laboratory of Radiation Medicine and Protection, Soochow University (GZK1202305, GZK1202203). All the funders were not involved in any aspect of the study design, data handling, manuscript preparation or publication decision.

Declarations

Conflict of interest

No potential conflict of interest was reported by the authors.

Additional information

Supplementary Information The online version contains supplementary material available at https://doi.org/10.1038/s41598-025-30716-9.

Correspondence and requests for materials should be addressed to X.W. or J.Z.